Pulse Power Boost Converter on Gallium Nitride Transistors

© E.A. Shershunova¹, S.I. Moshkunov¹, V.Yu. Khomich¹, A.A. Igolkin²

¹ Institute for Electrophysics and Electric Power of Russian Academy of Sciences,

191186 St. Petersburg, Russia ² Samara National Research University,

443086 Samara, Russia

E-mail: eshershunova@ieeras.ru

Received April 28, 2025 Revised July 16, 2025 Accepted July 23, 2025

A module of a pulse power boost DC/DC voltage converter with an output voltage of 130 V, a power of 3 kW and an operating frequency of 100 kHz on field-effect transistors based on gallium nitride has been developed and successfully tested. The power loss calculation on the elements of the power converter has been performed. The main mechanism of losses due to the heating of the crystal in the conduction state was revealed. The efficiency of the converter operating at maximum power was experimentally obtained to be 98.5 %, which coincided well with the calculation.

Keywords: voltage converter, aircraft, gallium nitride transistors, power losses.

DOI: 10.61011/SC.2025.05.61989.7906

A distributed hybrid power plant, which implies the use of electrical energy both from electrochemical power sources, such as a battery and fuel cells, and from a generator driven by an internal combustion engine, has been proposed as a means to increase the payload and flight range of light aircraft [1–3].

In the present study, we report on the design of a pulse power boost converter for a fuel cell. The converter is specific in utilizing a so-called synchronous circuit with high-mobility wide-bandgap gallium nitride power transistors used as two controlled switching elements.

The optimal operating voltage of the considered fuel cell is 90 V. However, since the output voltage of a fuel cell varies greatly with current and time [4,5], a boost converter with an input voltage of $90-130 \, \text{V}$ and an output voltage of $130 \, \text{V}$ (the optimal bus voltage for the used electric motor) has been designed and fabricated.

Figure 1 illustrates the operating principle of the boost converter. The photographic image of its power board is presented in the same figure. In distinction from the traditional circuit, another MOS transistor is used instead of a Schottky diode. The synchronous circuit provides an increase in efficiency through the suppression of losses at the top switching element. In addition, this circuit allows for more stable control of the converter due to the lack of an discontinuous current mode [6].

Output voltage V_o is formed over two phases where transistor Q_2 is conducting and Q_1 is non-conducting, and vice versa. When transistor Q_2 is in the conducting state, energy is accumulated in inductor L. When Q_1 is in ON-state, the energy stored in the inductor is transferred to capacitor C_o and load R_l . The ON-state and OFF-state time of the switches are defined using pulse width modulation (PWM), where the output voltage is specified by duty

factor D, which may be expressed, if losses are neglected, as $D = 1 - V_{in}/V_o = (V_o - V_{in})/V_o$.

Specifically, output voltage V_o at input $V_{\rm in}$ is obtained with switch Q_2 remaining open for $D \cdot T$ and switch Q_1 being open for $(1-D) \cdot T$, respectively, where T is the pulse period.

The input current through inductor L is defined as $I_{\rm in}=I_o/(1-D)$. The peak current is specified by pulsations $\Delta I=I_{\rm in}k$, which are taken to be $20-40\,\%$ of the average current value; i.e., k=0.3. $I_p=I+\Delta I/2$ is the peak current. The inductance may be determined as $L=V_{\rm in}\cdot D\cdot T/\Delta I$. A capacitor is needed to smooth the output voltage in the circuit. The corresponding capacitance may be calculated as $C_o=I_oDT/\Delta V_o$, where ripple voltage $\Delta V_o/2$ are taken to be $\leq 2\,\%$ of the voltage at the converter output.

The boost converter is controlled through the peak current of the bottom switch via a double current and voltage feedback loop [7,8]. The current through transistor Q_2 serves as a current feedback signal, while the output voltage acts as a voltage feedback signal. The current signal is taken from resistive sensor R_s with a total resistance of $10 \,\mathrm{m}\Omega$ that is connected in series with transistor Q_2 . For further processing, the signal from the current sensor is amplified by a factor of 10 (V_s) . Voltage signal V_{fb} is taken from the output voltage divider. The voltage error signal is the input signal of the PWM modulator, which also receives the signal from the current sensor. The generated PWM signal goes to the transistor driver. A UCC21225 isolated dual-channel power driver generates two control signals for transistors V_{g1} and V_{g2} at the output with a relative delay (tens to hundreds of ns) in response to the Disable signal. The control circuit supports a soft start mode and provides protection against false triggering.

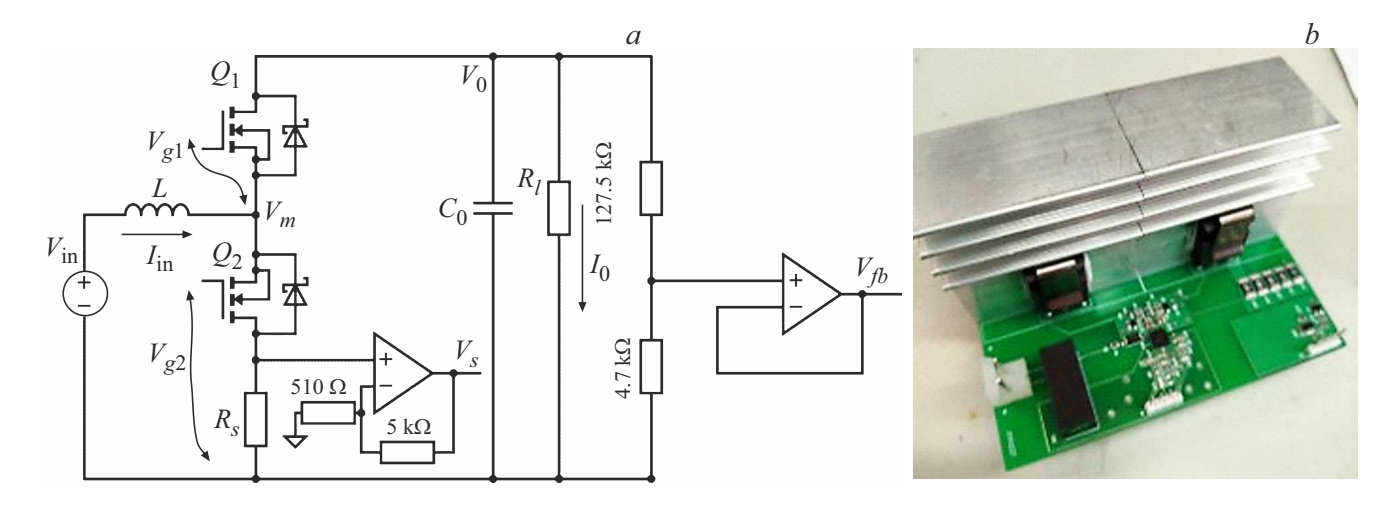


Figure 1. Pulse synchronous boost DC/DC voltage converter: a — operating principle; b — photographic image of the power board of the 3 kW module.

Voltage converter parameters

Parameter	Value
Input voltage $V_{\rm in}$, V	90-130
Output voltage V_o , V	130
Pulse frequency f , kHz	100
Inductor current I_{in} , A	33
Output current I_o , A	23
Inductance of the inductor $L, \mu H$	40
Capacitance of the output capacitor $C_o, \mu F$	14

The table lists the calculated parameters of the voltage converter.

Gallium nitride transistors (Nexperia GAN041-650WSB) were used as semiconductor switches. The output capacitance was composed of Suntan power film capacitors (680 nF, 400 V). The power inductor had a U-shaped airgapped ferrite core produced in Russia. Nine turns of PETV-2 enameled copper wire with a diameter of 2 mm were wound on the core. The air gap was 1 mm. The measured inductance was $42\,\mu\text{H}$, and the saturation current of the inductor was $48\,\text{A}$.

The procedure for optimization of the circuit and design detailed in [8] was used to calculate the losses of the module and its efficiency (ef) as functions of the input voltage in two cases: (i) with one transistor per arm (Figure 2, a); (ii) with two transistors per arm arranged in parallel (Figure 2, b).

The main sources of converter losses P_{los} are losses in the transistors, conduction losses P_{cond} due to onresistance R_{DSon} of the channel, and switching losses P_{sw} due to output capacitance C_{oss} of the transistor and reverse
recovery time t_{rr} of the diode. Power is also dissipated
in the inductor, which is associated with heating of the
wound wire, losses in the core, and losses attributable to
a reduction of the effective wire area due to the skin effect,

and in capacitors. According to calculated data, the total losses in the inductor do not exceed $8.3\,\mathrm{W}$, and the losses in the output capacitors are no greater than $0.2\,\%$ of the total power.

The obtained data indicate that the main contribution to power loss is made by transistor conduction losses, which are specified by the current through the transistor and its channel resistance R_{DSon} that increases with crystal temperature. Thus, both fine heat dissipation and a parallel connection of several transistors may contribute to an increase in efficiency (Figure 2, b).

Knowing the loss power per one transistor ($P_1 \le 25 \,\mathrm{W}$), the permissible crystal temperature ($T_j = 125 \,^{\circ}\mathrm{C}$), the ambient temperature ($T_a = 40 \,^{\circ}\mathrm{C}$), and the thermal resistances between the crystal and the case (R_{jc}) and between the case and the radiator (R_{cs}) and having determined thermal resistance R_{ja} between the crystal and the air by formula $R_{ja} = (T_j - T_a)/P_1$, we find the required thermal resistance of the radiator R_{sa} as $R_{sa} = R_{ja} - R_{jc} - R_{cs}$ [9]. Inserting the numerical values, we obtain $R_{sa} = 2.3 \,^{\circ}\mathrm{C/W}$ and a permissible temperature difference between the radiator and the air of 57.5 $\,^{\circ}\mathrm{C}$. With forced ventilation cooling, this figure may be increased. A Fisher S514-50 radiator with a thermal resistance of 3.5 $\,^{\circ}\mathrm{C/W}$ with forced air cooling at a velocity of 4 m/s satisfies these requirements. A correction factor of 0.6 is thus introduced [10].

The fabricated module was tested in various modes. In these tests, current $I_{\rm in}$ from the source and current I_o through the load were measured using 75ShSM current shunts with a 75 A rating and a 1 A/mV coefficient, and the input and output voltages were measured with Fluke 17B+ multimeters. A Rigol MS08104 digital oscilloscope was used to record V_{g1} and V_{g2} at the gates of transistors, signal V_s from the current sensor that represents the current through transistor Q_2 , middle point voltage V_m , and signals $V_{\rm in}$ and V_o .

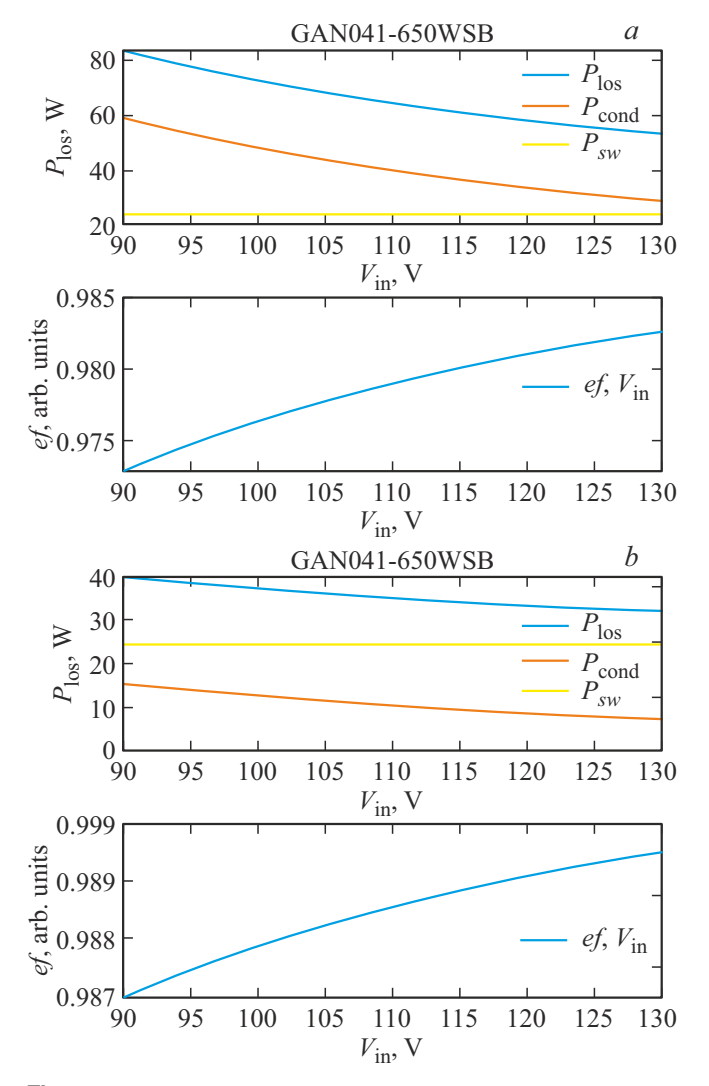


Figure 2. Calculated loss power in transistors P_{los} and efficiency ef of the converter with one transistor per arm (a) and with two transistors per arm arranged in parallel (b) at a crystal temperature of $100\,^{\circ}\text{C}$.

Figure 3 shows the typical oscilloscope records of voltages and signal V_s from the current sensor at a voltage of 90 V at the converter input. It was found that the converter operation remained stable regardless of the load and the transistor case temperature didn't not exceed 60 °C at maximum operating power. However, the output voltage ripple was slightly above the calculated level, which was apparently attributable to a change in ESR of the capacitors due to operation at a high frequency with high pulse currents.

It can be seen from Figure 4 that the experimentally determined dependence of efficiency of the converter operating at maximum power on the input voltage is quantitatively similar to the calculated one (Figure 2, a).

The designed 3 kW module is compact, has high efficiency, which may be improved by arranging a parallel connection of two transistors per arm, and offers current

and voltage stabilization. Connecting several such modules, one may build converters with a power of tens of kilowatts, high efficiency, and a high power-to-weight ratio, which is important for use aboard spacecraft.

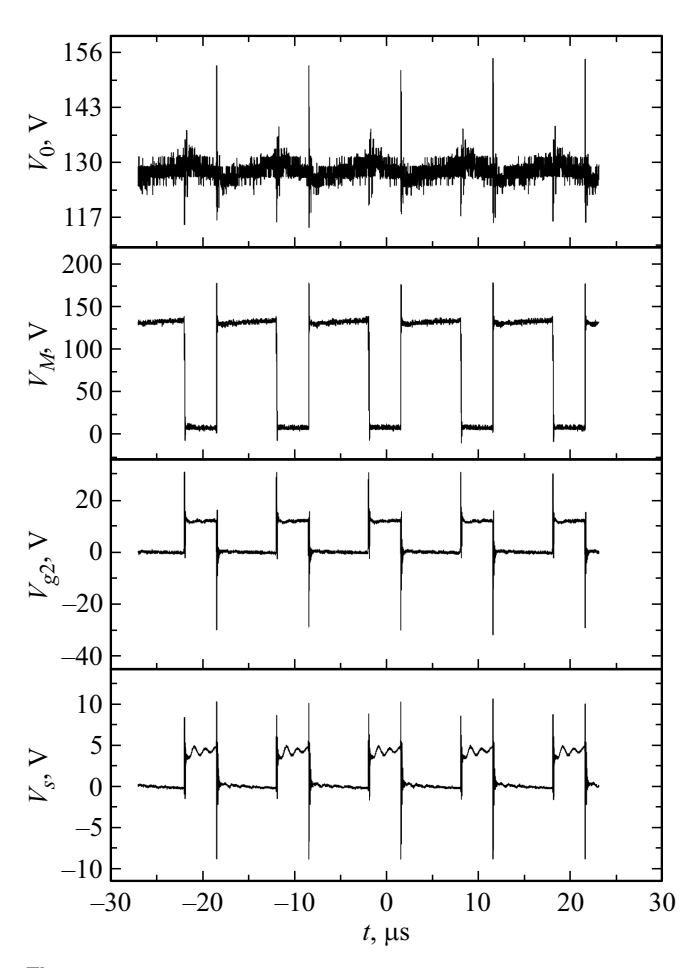


Figure 3. Oscilloscope records of voltages at the maximum operating power of 3 kW and $V_{\rm in} = 90 \, \text{V}$: V_o — output voltage, V_m — middle point voltage, V_{g2} — gate voltage of Q_2 , and V_s — signal from the current sensor $(10 \, \text{A/V})$.

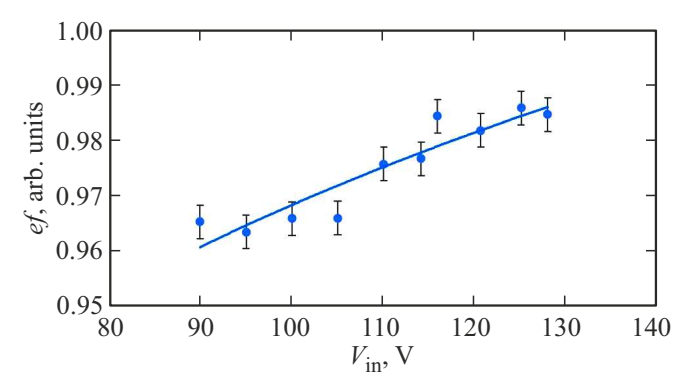


Figure 4. Experimentally determined efficiency of the $3 \,\mathrm{kW}$ converter module as a function of voltage at its input V_{in} (one transistor per arm).

Funding

This study was supported financially by the Ministry of Education and Science of the Russian Federation, agreement No. 075-15-2024-558.

Conflict of interest

The authors declare that they have no conflict of interest.

References

- B.J. Brelje, J.R. Martins. Progr. Aerospace Sci., 104, 1 (2019). DOI: 10.1016/j.paerosci.2018.06.004
- [2] T. Lei, Z. Min, Q. Gao, L. Song, X. Zhang. Energies, 15 (11), 4109 (2022). DOI: 10.3390/en15114109
- [3] M.A. Rendón, R.C.D. Sánchez, M.J. Gallo, A.H. Anzai. J. Control, Automation and Electrical Systems, 32 (5), 1244 (2021). DOI: 10.1007/s40313-021-00740-x
- [4] A.A. Belmesov, L.V. Shmygleva, A.A. Baranov, A.V. Levchenko. Russ. Chem. Rev., 93 (6), RCR5121 (2024). DOI: 10.59761/RCR5121
- [5] A.A. Ferreira, J.A. Pomilio, G. Spiazzi, Silva L de Araujo. IEEE Trans. Power Electron., 23 (1), 107 (2008). DOI: 10.1109/TPEL.2007.911799
- [6] Understanding Boost Power Stages in Switch Mode, Application Report (Texas Instruments, March 1999).
- [7] S.I. Moshkunov, V.Yu. Khomich, E.A. Shershunova. Tech. Phys. Lett., 46 (8), 749 (2020).
 DOI: 10.21883/PJTF.2020.15.49743.18139
- [8] A.N. Varyukhin, M.V. Gordin, A.V. Dutov, S.I. Moshkunov,
 V.Yu. Khomich, E.A. Shershunova. Prikl. Fiz., 1, 75 (2021).
 (in Russian). DOI: 10.51368/1996-0948-2021-1-75-81
- [9] A. Kolpakov. Kompon. Tekhnol., 18, 46 (2002). (in Russian).
- [10] S.L. Koryakin-Chernyak, O.N. Partala, Yu.N. Davidenko, V.Ya. Volodin. *Elektrotekhnicheskii spravochnik* (SPb., Nauka Tekh., 2009), p. 456 (in Russian).

Translated by D.Safin